

Interlayer interaction in multilayer [Co/Pt]*n*/Pt/Co structures

E. S. Demidov, N. S. Gusev, L. I. Budarin, E. A. Karashtin, V. L. Mironov, and A. A. Fraerman

Citation: *Journal of Applied Physics* **120**, 173901 (2016); doi: 10.1063/1.4967163

View online: <http://dx.doi.org/10.1063/1.4967163>

View Table of Contents: <http://scitation.aip.org/content/aip/journal/jap/120/17?ver=pdfcov>

Published by the [AIP Publishing](#)

Articles you may be interested in

[The role of the non-magnetic material in spin pumping and magnetization dynamics in NiFe and CoFeB multilayer systems](#)

J. Appl. Phys. **117**, 163901 (2015); 10.1063/1.4918909

[Spin polarization of currents in Co/Pt multilayer and Co–Pt alloy thin films](#)

Appl. Phys. Lett. **97**, 022505 (2010); 10.1063/1.3460910

[Correlation between perpendicular exchange bias and magnetic anisotropy in IrMn/\[Co/Pt\]*n* and \[Pt/Co\]*n*/IrMn multilayers](#)

J. Appl. Phys. **97**, 063907 (2005); 10.1063/1.1861964

[Structural, magnetic, and spectroscopic magneto-optical properties aspects of Pt–Co multilayers with intentionally alloyed layers](#)

J. Appl. Phys. **94**, 7662 (2003); 10.1063/1.1629156

[Exchange decoupling of grains in polycrystalline CoPt alloy films \(abstract\)](#)

J. Appl. Phys. **81**, 3845 (1997); 10.1063/1.364728

Interlayer interaction in multilayer [Co/Pt]_n/Pt/Co structures

E. S. Demidov,¹ N. S. Gusev,² L. I. Budarin,¹ E. A. Karashtin,^{1,2} V. L. Mironov,^{1,2} and A. A. Fraerman^{1,2}

¹University of Nizhny Novgorod, 23 Prospekt Gagarina, 603950 Nizhny Novgorod, Russia

²Institute for Physics of Microstructures RAS, GSP-105, 603950 Nizhny Novgorod, Russia

(Received 10 June 2016; accepted 22 October 2016; published online 3 November 2016)

We report a study of interlayer exchange interaction in multilayer [Co/Pt]_n/Pt/Co structures. The structures consist of a periodic [Co/Pt]_n multilayer film with a perpendicular anisotropy and a thick Co layer with an in-plane anisotropy. The subsystems are separated by a Pt spacer with variable thickness. The magneto-optical Kerr effect and the ferromagnetic resonance measurements show the essentially non-collinear state of magnetic moments of the layers and strong exchange coupling between the [Co/Pt]_n and the Co subsystems. A simple model based on the Landau-Lifshitz-Gilbert equation shows that the exchange coupling is ferromagnetic. The exchange constant is estimated in this simple model. The estimated value is $J = 2 \text{ erg/cm}^2$. Published by AIP Publishing. [<http://dx.doi.org/10.1063/1.4967163>]

I. INTRODUCTION

Thin magnetic films and multilayer structures with a perpendicular anisotropy are the subject of intensive research driven by promising applications in the modern magnetic data storage systems. In the recent years, much attention has been paid to multilayer systems based on the thin Co layers separated by metal spacers M (such as Pt, Pd, Ni, Au, and Ag).¹⁻⁶ Perpendicular anisotropy in these systems is a property of the Co/M interface.² If Co layer thickness is less than a critical value ($\sim 1 \text{ nm}$), surface anisotropy exceeds shape anisotropy and the multilayer Co/M system is perpendicularly magnetized. This property of Co/M multilayers considerably expands the opportunities in the development of magneto-optical and magnetoresistive devices with the lateral/vertical architecture.⁷⁻⁹

Over the last few years, the properties of exchange coupled systems with distinct anisotropy directions have been actively investigated.¹⁰⁻²¹ In particular, the [Co/Pt]_n/F structures that consist of [Co/Pt]_n multilayer film with a perpendicular anisotropy and ferromagnetic layer (F) with an in-plane anisotropy have been proposed to control the hysteresis loop shift (exchange bias) of magnetic system.¹³⁻¹⁵ Besides, the patterned [Co/Pt]_n/F structures were recently used to create artificial magnetic skyrmion states.¹⁶⁻²³ Note that the effects of the exchange bias and skyrmion nucleation are based on the existence of strong exchange interaction in both between Co layers in [Co/Pt]_n film and between [Co/Pt]_n film and ferromagnetic layer F. There are some indirect investigations of exchange coupling in similar systems: e.g., the exchange constant in the [Co/Pt]_n multilayers was recently determined from the transport measurements.²⁴ It is supposed that there is the exchange interaction that is mainly of RKKY origin.²⁴ However, no direct experimental studies have been so far performed. The aim of this work is the study of the interlayer exchange interaction in the multilayer [Co/Pt]_n/Pt/Co structures ($n = 5$) by the ferromagnetic resonance (FMR) method.

II. EXPERIMENTAL METHODS AND RESULTS

The [Co(0.9 nm)Pt(1.5 nm)]₅/Pt(*d*)/Co(10 nm) structures (further denoted as [Co/Pt]₅/Pt(*d*)/Co) with different spacer thicknesses $d = 0$ and $d = 1.5 \text{ nm}$ (see Fig. 1) are grown by

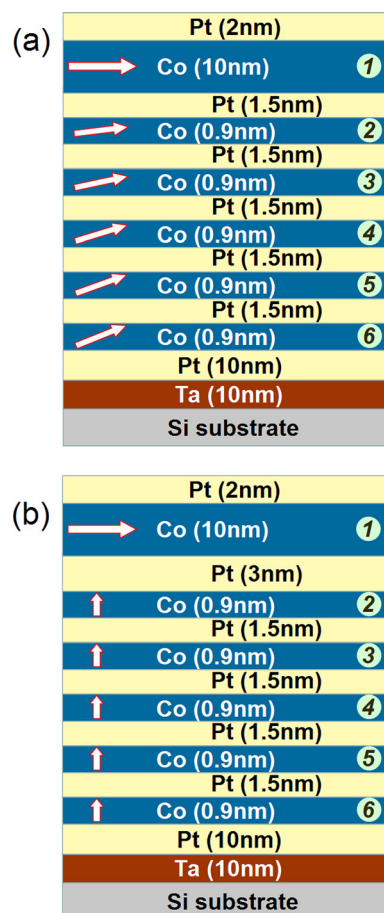


FIG. 1. A schematic drawing of (a) the [Co/Pt]₅/Pt(0)/Co and (b) the [Co/Pt]₅/Pt(1.5)/Co multilayer structures. The numbers of the layers are shown on the right side; the arrows on the left side demonstrate the non-collinear magnetization distribution.

dc magnetron sputtering on an Si substrate.²¹ The Ta(10 nm) and Pt(10 nm) underlayers were used to improve the properties of the [Co/Pt]₅ multilayers with a perpendicular anisotropy. In addition, a multilayer [Co(0.9 nm)Pt(1.5 nm)]₅ structure and a Co(10 nm) film are grown separately on similar substrates. The thickness of the layers is determined with the Bruker diffractometer (wavelength $\lambda = 0.154$ nm) by the small-angle X-ray scattering method. The magnetization curves of the samples are measured by polar magnetooptical Kerr effect (MOKE) (He-Ne laser has 628 nm irradiation wavelength, and the applied magnetic field is perpendicular to the layers plane). The residual sample domain structure is studied using the vacuum magnetic force microscope (MFM) “Solver-HV” (NT-MDT Company). The standard NSG-11 cantilever with Co coating is used as the MFM probe. The measurements are performed in the constant-height mode with the MFM contrast proportional to the phase shift of the cantilever oscillations under the gradient of magnetic force.^{25,26}

The FMR measurements are performed using the Bruker EMX Plus-10/12 spectrometer equipped by a dc magnet with field H up to 15 kOe. Polarized microwave magnetic field \mathbf{h} at 9.8 GHz frequency (TE_{011} mode of resonant cavity) is perpendicular to the zero-frequency magnetic field \mathbf{H} . The samples are driven through resonance by sweeping the magnitude of magnetic field H . The dependences of the resonant magnetic field H_r on the angle θ_H between \mathbf{H} and the normal to the plane are investigated by rotating the sample around the axis parallel to the direction of magnetic component of microwave field \mathbf{h} .

The MOKE curves for [Co/Pt]₅/Pt(0)/Co and [Co/Pt]₅/Pt(1.5 nm)/Co are shown in Figs. 2(a) and 2(b), respectively. The magnetization curve of the [Co(0.9 nm)Pt(1.5 nm)]₅ sample is shown by the dashed line in Fig. 2(a). Note that the remanence magnetization is less than the magnetization in the saturation due to splitting into domains, which is confirmed by the MFM measurements (inset in Fig. 2(a)). The magnetization curve of the [Co/Pt]₅/Pt(0)/Co sample is hysteresis-less. It is essentially different in comparison with the curve of the [Co(0.9 nm)Pt(1.5 nm)]₅ sample. In contrast, the magnetization curve of [Co/Pt]₅/Pt(1.5 nm)/Co sample keeps hysteresis, although having distinctions from that of [Co/Pt]₅ without a thick Co capper. This is attributed to small influence of the thick Co layer on the [Co/Pt]₅ subsystem. Significant change of the magnetic properties of the multilayer [Co/Pt]₅ structure caused by the thick cobalt film in the [Co/Pt]₅/Pt(0)/Co sample is supposed to appear due to the interaction between these subsystems through a platinum spacer. We use the FMR method in order to study this effect in detail.

The dependence of the resonant magnetic field H_r on the angle θ_H between \mathbf{H} and the normal to the plane for the Co(10 nm) film and the multilayer [Co(0.9 nm)Pt(1.5 nm)]₅ structure is shown in Fig. 3(a). The FMR signal is invariant with respect to the in-plane rotation of the investigated structures. So the lateral anisotropy is also neglected in the calculations. Let us compare the resonant field for the separate Co(10 nm) film and for the [Co(0.9 nm)Pt(1.5 nm)]₅ structure (see Fig. 3(a)). We see that the thick cobalt film has in-plane

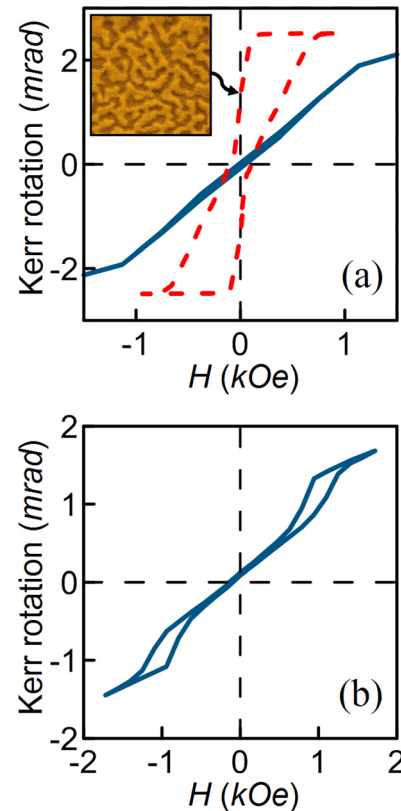


FIG. 2. Polar MOKE magnetization curves of the samples. (a) The hysteresis loop of CoPt/Pt(0)/Co (solid line; blue online) and [Co(0.9 nm)Pt(1.5 nm)]₅ (dashed line; red online). The inset represents an MFM image of the residual state of [Co(0.9 nm)Pt(1.5 nm)]₅ sample, with a frame size of 3 μ m. (b) The hysteresis loop of CoPt/Pt(1.5 nm)/Co.

anisotropy, while the [Co/Pt]₅ multilayer structure is a magnetic system with a perpendicular anisotropy.

The angular dependences of the resonant field for the [Co/Pt]₅/Pt(0)/Co sample with thin spacer (1.5 nm total) between [Co/Pt]₅ and Co are shown in Fig. 3(b). We observe a large splitting for two branches of the resonant oscillations, which is a direct evidence of strong interaction between the subsystems. Angular dependences for the sample with thick Pt spacer (3 nm total, $d = 1.5$ nm) between Co and [Co/Pt]₅ (the crosses and pluses in Fig. 3(b)) are different. In this case, there are two almost independent subsystems. Simple estimations show that such dependence of $H_r(\theta_H)$ splitting on the thickness of the Pt spacer cannot be explained by the magnetostatic interaction mechanism.²⁷ Therefore, we suppose the existence of the exchange interaction between the Co and the [Co/Pt]₅ subsystems.

III. DISCUSSION

We consider the following simple model to estimate the value of the exchange interaction in the [Co/Pt]₅/Pt(0)/Co sample. The magnetization \mathbf{M}_i of the i -th Co layer (see Fig. 1) is uniform throughout the layer. \mathbf{M}_i lies in a plane formed by the vectors of normal and external magnetic field \mathbf{H} ; its orientation is determined by the angle θ_i with respect to the normal to layers. Saturation magnetization M was considered to be equal to the volume value²⁸ of 1420 G for all the Co layers. The effective anisotropy of each cobalt layer is determined by

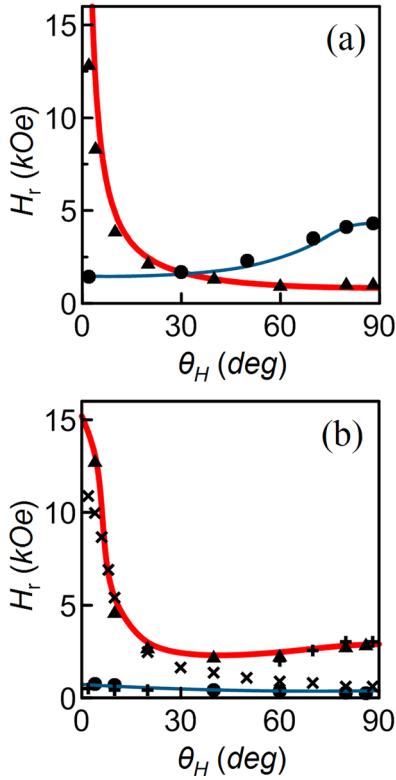


FIG. 3. The angular dependences of the resonant field position $H_r(\theta_H)$ (a) for the Co layer (experimental black triangles and calculated thick line (red online)) and for the $[\text{Co}(0.9\text{nm})\text{Pt}(1.5\text{nm})]_5$ structure (experimental black circles and calculated thin line (blue online)); (b) for the $[\text{Co}/\text{Pt}]_5/\text{Pt}(0)/\text{Co}$ sample, acoustic mode (experimental black triangles and calculated thick line (red online)) and optical mode (experimental black circles and calculated thin line (blue online)). The crosses and pluses in (b) are the experimental data for two modes in the $[\text{Co}/\text{Pt}]_5/\text{Pt}(1.5\text{nm})/\text{Co}$ sample.

the interplay of the uniaxial anisotropy and the demagnetizing factor. Assuming that the value of uniaxial anisotropy depends only on the layer thickness, we take equal anisotropy constant K for layers 2–6 and a different constant K_c for thick Co layer 1. We also use the equal constants of exchange interaction between all neighbour cobalt layers since the platinum interlayers between them have the same thickness in the considered structure. Then, the expression for surface energy density can be written in the following form

$$E = (2\pi M^2 - K_c)l_1 \cos^2\theta_1 + (2\pi M^2 - K) \sum_{i=2}^6 l_i \cos^2\theta_i - \sum_{i=1}^6 l_i \mathbf{H} \cdot \mathbf{M}_i - \frac{J}{M^2} \sum_{i=1}^5 \mathbf{M}_i \cdot \mathbf{M}_{i+1}, \quad (1)$$

where l_i is the i -th layer thickness and J is the interlayer exchange interaction constant (per unit area). Note that in our simple model we neglect the magnetostatic interaction between the layers that may appear due to surface roughness (the so-called Néel “orange peel” coupling²⁹). Taking into account the magnetostatic interaction would lead to a small correction of the parameters estimated below and is beyond the scope of the current paper.

Dynamics of the magnetization vectors is described by the system of Landau-Lifshitz-Gilbert equations

$$\frac{\partial \mathbf{M}_i}{\partial t} = -\gamma_i [\mathbf{M}_i \times \mathbf{H}_i] + \frac{\alpha}{M} [\mathbf{M}_i \times [\mathbf{M}_i \times \mathbf{H}_i]], \quad (2)$$

where $\mathbf{H}_i = -\frac{\partial E}{\partial \mathbf{M}_i}$ is the effective magnetic field acting on the i -th ferromagnetic layer (determined by (1)) and γ_i is the gyromagnetic ratio that is slightly different for $[\text{Co}/\text{Pt}]_5$ and Co due to different g -factor. The parameter α in (2) is the damping constant, which generally determines the width of FMR lines. The dependences of resonant fields on the system parameters are determined by the system (2) linearized in the vicinity of the equilibrium state ($[\mathbf{H}_i \times \mathbf{M}_i] = 0$). We acquire the best fit of experimental data with the following parameters: $K = 1.36 \times 10^7 \text{ erg/cm}^3$; $K_c = 4 \times 10^6 \text{ erg/cm}^3$; $J = 2 \text{ erg/cm}^2$; $g_1 = 2$; $g_{2-6} = 2.07$ (g_i is a g -factor that determines γ_i). Let us note that our experimental estimation of the exchange constant J has the same order of value, as obtained previously in the transport measurements.²⁴ The difference in the values can be attributed to slightly different Pt spacer thickness and to possible difference in other parameters such as surface quality. Calculated dependences of resonant fields on the angle θ_H are shown with the solid lines in Fig. 3. The effective anisotropy of the cobalt layers in the multilayer $[\text{Co}/\text{Pt}]_5$ structure ($i = 2..6$) ($2\pi M^2 - K$) $\approx -1.3 \times 10^6 \text{ erg/cm}^3$ is negative (perpendicular anisotropy) and the effective anisotropy of thick Co film ($2\pi M^2 - K_c$) $\approx 8.7 \times 10^6 \text{ erg/cm}^3$ is positive (in-plane anisotropy).

The exchange interaction between the subsystems with different anisotropy types leads to the collective magnetization oscillations. The calculations show that the high-field and the low-field branches correspond to the cophased and antiphased oscillations of the magnetic moments of the thick Co film and the layers of the multilayer $[\text{Co}/\text{Pt}]_5$ structure, respectively. So the exchange interaction between the subsystems is of ferromagnetic type ($J > 0$). The corresponding effective exchange field H_{ex} is $H_{ex} \sim 16 \text{ kOe}$.

We believe that the mechanism of the exchange interaction is RKKY.²⁴ It leads to the non-collinear magnetization distribution characterized by the magnetic moments lying

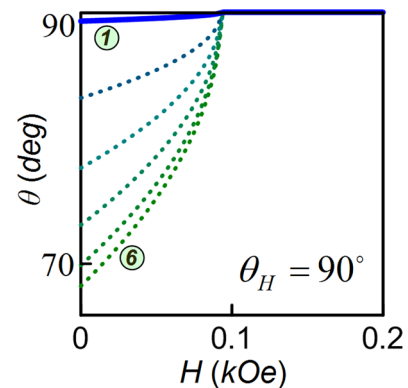


FIG. 4. The dependences of the equilibrium angles of magnetic moments θ_i of the layers on the external magnetic field applied along the $[\text{Co}/\text{Pt}]_5/\text{Pt}(0)/\text{Co}$ sample plane. The thick curve corresponds to the Co(10nm) layer, and the thin dotted curves correspond to the Co layers in the $[\text{Co}/\text{Pt}]_5$ multilayer in order of increasing distance from the thick Co layer.

neither in layers plane nor perpendicular to them (schematically shown in Fig. 1). The results of the calculations of the equilibrium magnetic states under the applied in-plane magnetic field for $[\text{Co}/\text{Pt}]_5/\text{Pt}(0)/\text{Co}$ sample are shown in Fig. 4. We see that the angle between the magnetic moment and the normal to the sample increases with the number of layers. This distribution is very similar to that demonstrated by thin films with different types of surface and volume anisotropy.^{30–33}

IV. CONCLUSION

In summary, the FMR investigation of the multilayer $[\text{Co}/\text{Pt}]_n/\text{Pt}/\text{Co}$ structure ($n=5$) is carried out. The structure consists of a thick Co layer with an in-plane anisotropy and a periodic $[\text{Co}/\text{Pt}]_n$ film with a perpendicular anisotropy. Strong exchange interaction between Co and $[\text{Co}/\text{Pt}]_n$ subsystems is found in the case of a thin platinum spacer (1.5 nm). The interaction is practically absent in the system with a thick spacer (3 nm). This shows that variation of the interlayer spacing enables an effective control of non-collinear states in such systems. The exchange interaction between the subsystems gives an opportunity to create artificial structures with a non-collinear magnetization distribution. For example, a Néel-type magnetic structure may be fabricated in which the magnetic moment has a component along the direction of its change. These structures are of certain interest for the experimental observation of the flexo-magnetoelectric effect that was predicted in the non-collinear systems.³⁴

ACKNOWLEDGMENTS

The authors are thankful to O. L. Ermolaeva and M. V. Sapozhnikov for the valuable discussions.

Sample fabrication and MOKE investigations were supported by the Russian Science Foundation (Grant No. 16-12-10340). MFM and FMR measurements were supported by the Russian Science Foundation (Grant No. 16-12-10254). Theoretical calculations were supported by the Russian Foundation for Basic Research. E.S.D. would like to thank the program “Development of the Scientific Potential of Higher Education,” Project No. 02V.49.21.0003 of the Nizhny Novgorod State University.

¹R. Sbiaa, H. Meng, and S. N. Piramanayagam, *Phys. Status Solidi RRL* **5**, 413 (2011).

²P. F. Carcia, A. D. Meinhardt, and A. Suna, *Appl. Phys. Lett.* **47**, 178 (1985).

³P. F. Carcia, *J. Appl. Phys.* **63**, 5066 (1988).

⁴G. H. O. Daalderop, P. J. Kelly, and F. J. A. den Broeder, *Phys. Rev. Lett.* **68**, 682 (1992).

⁵F. J. A. den Broeder, D. Kuiper, A. P. van de Mosselaer, and W. Hoving, *Phys. Rev. Lett.* **60**, 2769 (1988).

⁶G. N. Kakazei, P. P. Martin, A. Ruiz, M. Varela, M. Alonso, E. Paz, F. J. Palomares, F. Cebollada, R. M. Rubinger, M. C. Carmo, and N. A. Sobolev, *J. Appl. Phys.* **103**, 07B527 (2008).

⁷R. L. Stamps, S. Breitkreutz, J. Åkerman, A. V. Chumak, Y. Otani, G. E. W. Bauer, J.-U. Thiele, M. Bowen, S. A. Majetich, M. Klaui, I. L. Prejbeanu, B. Dieny, N. M. Dempsey, and B. Hillebrands, *J. Phys. D: Appl. Phys.* **47**, 333001 (2014).

⁸W. B. Zeper, H. W. van Kesteren, B. A. J. Jacobs, J. H. M. Spruit, and P. F. Carcia, *J. Appl. Phys.* **69**, 4966 (1991).

⁹Z. Kugler, J.-P. Grote, V. Drewello, O. Schebaum, G. Reiss, and A. Thomas, *J. Appl. Phys.* **111**, 07C703 (2012).

¹⁰L. Tryputen, F. Guo, F. Liu, T. N. A. Nguyen, M. S. Mohseni, S. Chung, Y. Fang, J. Åkerman, R. D. McMichael, and C. A. Ross, *Phys. Rev. B* **91**, 014407 (2015).

¹¹T. N. A. Nguyen, Y. Fang, V. Fallahi, N. Benatmane, S. M. Mohseni, R. K. Dumas, and J. Åkerman, *Appl. Phys. Lett.* **98**, 172502 (2011).

¹²S. Tacchi, T. N. A. Nguyen, G. Carlotti, G. Gubbiotti, M. Madami, R. K. Dumas, J. W. Lau, J. Åkerman, A. Rettori, and M. G. Pini, *Phys. Rev. B* **87**, 144426 (2013).

¹³A. Bollero, L. D. Buda-Prejbeanu, V. Baltz, J. Sort, B. Rodmacq, and B. Dieny, *Phys. Rev. B* **73**, 144407 (2006).

¹⁴A. Bollero, V. Baltz, L. D. Buda-Prejbeanu, B. Rodmacq, and B. Dieny, *Phys. Rev. B* **84**, 094423 (2011).

¹⁵W. J. Gong, W. Liu, X. H. Liu, S. Guo, J. N. Feng, B. Li, and Z. D. Zhang, *J. Appl. Phys.* **109**, 043906 (2011).

¹⁶N. Nagaosa and Y. Tokura, *Nat. Nanotechnol.* **8**, 899 (2013).

¹⁷L. Sun, R. X. Cao, B. F. Miao, Z. Feng, B. You, D. Wu, W. Zhang, A. Hu, and H. F. Ding, *Phys. Rev. Lett.* **110**, 167201 (2013).

¹⁸B. F. Miao, L. Sun, Y. W. Wu, X. D. Tao, X. Xiong, Y. Wen, R. X. Cao, P. Wang, D. Wu, Q. F. Zhan, B. You, J. Du, R. W. Li, and H. F. Ding, *Phys. Rev. B* **90**, 174411 (2014).

¹⁹M. V. Sapozhnikov and O. L. Ermolaeva, *Phys. Rev. B* **91**, 024418 (2015).

²⁰M. V. Sapozhnikov, *J. Magn. Magn. Mater.* **396**, 338 (2015).

²¹A. A. Fraerman, O. L. Ermolaeva, E. V. Skorohodov, N. S. Gusev, V. L. Mironov, S. N. Vdovichev, and E. S. Demidov, *J. Magn. Magn. Mater.* **393**, 452 (2015).

²²R. H. Liu, W. L. Lim, and S. Urazhdin, *Phys. Rev. Lett.* **114**, 137201 (2015).

²³M. V. Sapozhnikov, S. N. Vdovichev, O. L. Ermolaeva, N. S. Gusev, A. A. Fraerman, S. A. Gusev, and Y. V. Petrov, *Appl. Phys. Lett.* **109**, 042406 (2016).

²⁴M. Bersweiler, D. Lacour, K. Dumesnil, F. Montaigne, and M. Hehn, *Phys. Rev. B* **92**, 224431 (2015).

²⁵A. Thiaville, J. Miltat, and J. M. Garcia, *Magnetic Microscopy of Nanostructures*, edited by H. Hopster and H. P. Oepen (Springer-Verlag, 2005).

²⁶V. L. Mironov, O. L. Ermolaeva, E. V. Skorohodov, and A. Y. Klimov, *Phys. Rev. B* **85**, 144418 (2012).

²⁷B. D. Schrag, A. Anguelouch, G. Xiao, P. Trouilloud, Y. Lu, W. J. Gallagher, and S. S. P. Parkin, *J. Appl. Phys.* **87**, 4682 (2000).

²⁸A. P. Babichev, N. A. Babushkina, A. M. Bratkovskiy *et al.*, *Physical Quantities*, edited by I. S. Grigoriev and E. Z. Meilikhov (Energoatomizdat, Moscow, 1991).

²⁹L. Néel, *C. R.* **255**, 1676 (1962).

³⁰D. L. Mills, *Phys. Rev. B* **39**, 12306 (1989).

³¹R. Allenspach, M. Stampanoni, and A. Bischof, *Phys. Rev. Lett.* **65**, 3344 (1990).

³²G. Bochi, C. A. Ballentine, H. E. Inglesfield, C. V. Thompson, and R. C. O’Handley, *Phys. Rev. B* **53**, R1729 (1996).

³³X. Hu and Y. Kawazoe, *Phys. Rev. B* **51**, 311 (1995).

³⁴V. G. Bar’yakhtar, V. A. L’vov, and D. A. Yablonskii, *JETP Lett.* **37**, 673 (1983).